

A THEORETICAL MODEL FOR EVALUATING REAL MEDIUM EFFECTS OF STEAM FLOW THROUGH PIPES

N.H. Mahmoud* and A. Abdel - Fattah**

* Associate Professor, ** Lecturer, Dept. of Mech. Power Eng., Faculty of Engineering, Menoufia University, Shebin El-Kom, Egypt.

ABSTRACT

This paper describes a theoretical model that considers the real medium effects on steam flow characteristics through pipes at high, moderate and low pressures. The present model utilizes two commonly used equations of state, namely the Beattie-Bridgeman (BB) equation and the second virial (SV) one. Modified basic equations are used in the model derivation in order to combine the effect of pipe roughness. Predictions for pressure, temperature and Mach number variations of steam flow along a pipe of such geometry were obtained using Runge-Kutta method in solving the model differential equations. Plots of results, however, include the corresponding variations in steam flow parameters when applying the perfect gas equation of state.

An experimental program was conducted to acquire experimental data. The computed results of steam flow pressure drop over the whole length of the pipe agreed well with the measurements of present experiments as well as the experimental data cited in the literature.

KEYWORDS

Real medium, steam flow characteristics, pipe flow, state equation, friction coefficient, pressure drop.

INTRODUCTION

Recently, complexity appeared in the flow diagrams of power plants due to using intermediate superheating and steam at high pressures can influence the design of plant piping system during the course of composing multiline piping with different nominal sizes [1]. Steam flow through pipe lines of power plants is mainly a two-phase flow. Theoretical correlations predicting the pressure gradients during the flow of two-phase, steam-water mixtures in smooth pipes [2] and rough ones [3] were carried out previously. The

*MANUSCRIPT RECEIVED FROM DR: N. H. Mahmoud, AT: 25/ 11/ 1996,
ACCEPTED AT: 27/ 12/ 1996, PP. 29-47,
ENGINEERING RESEARCH BULLETIN, VOL. 20, NO. 2, 1997,
MENOUIYA UNIVERSITY, FACULTY OF ENGINEERING,
SHEBIN EL-KOM, EGYPT. ISSN. 1110-1180.*

uncertainty which was caused by non-ideal (or real) gas considerations tends to lowering the degree of agreement between the experimental and theoretical results of steam flow characteristics through such devices, through converging-diverging nozzles under high pressure conditions. This analysis incorporates the Redlich-Kwong equation of state. Bober and Chow developed this model lately [5] to determine the effects of non-ideal gas behavior on the expansion factor, and consequently the mass flow rate, for the venturi meter [6]. A similar technique utilizes a truncated virial equation of state [7] was used by Bakhtar and others [8] in treating nucleation phenomena in flowing high pressure steam and by Sabry et al. [9] to simulate the expansion of nonequilibrium condensing wet steam at moderate and low pressures through nozzles.

In the present paper, a theoretical model describes real steam flow through pipes at low, moderate and high pressure is obtained. This model is based upon Beattie-Bridgeman formulation [10] for a state equation. This equation possess simplicity and reduces the computation time besides verifying higher degrees of accuracy. Besides, the model utilizes also a second- virial (SV) equation for steam state in evaluating the differences in the predicted flow parameters when using another equation for steam state. Furthermore, modified governing equations are used in the present analysis in order to quantify the effect of pipe roughness.

THEORETICAL MODEL

Figure 1 indicates an element of flow configuration through the pipe. This configuration considers a straight horizontal pipe of diameter D and of length L supplies steam flow of P_i, T_{gi}, ρ_i and M_{gi} , and delivers the same rate of steam flow at final conditions of P_b, T_{gb}, ρ_b and M_{gb} . Assumptions are made in deriving the basic equations of steam flow through the pipe as follows :

- a- The flow is one-dimensional.
- b- Steam specific heats at constant pressure and constant volume are considered to vary with both density and temperature.
- c- Steam is submitted to the real flow considerations as given in standard steam tables.
- d- Friction coefficient of the steam flow through the pipe is independent of Reynolds number.
- e- Steam flow is adiabatic.

Equations of conservation of mass, momentum and energy are written as follows :

$$VA\rho = \text{constant} \quad \text{or} \quad V\rho = \text{constant} \quad (1)$$

$$-\frac{dP}{\rho} - \frac{fL}{D} \cdot \frac{V^2}{2} = V \cdot dV \quad (2)$$

$$dh + V.dV = 0 \quad \text{or} \quad dh = T_g ds + v.dP \quad (3)$$

Rearranging equations (1) and (3) gives:

$$\frac{dV}{d\rho} = -\frac{V}{\rho} \quad (4)$$

$$dh = C_v.dT_g + T_g.\left(\frac{\partial P}{\partial T_g}\right)_v.dv + v.dP \quad (5)$$

Substituting dP from eq. (2) into eq. (5) and considering assumption (e) from the assumptions listed above yields:

$$\begin{aligned} dh &= -V.dV \\ &= C_v.dT_g + T_g.\left(\frac{\partial P}{\partial T_g}\right)_v.dv - \left(v.dV + \frac{fLV^2}{2D}\right) \\ \therefore C_v.dT_g + T_g.\left(\frac{\partial P}{\partial T_g}\right)_v.dv - \frac{fLV^2}{2D} &= 0 \end{aligned} \quad (6)$$

Dividing by dv and using differentiation of the inverse relation between v and ρ for such a gas, equation (6) becomes

$$C_v.\frac{dT_g}{(-d\rho/\rho^2)} + T_g.\left(\frac{\partial P}{\partial T_g}\right)_v - \frac{fLV^2}{2D.(-d\rho/\rho^2)} = 0 \quad (7)$$

Now, one can write the energy equation in the following form:

$$\frac{dT_g}{d\rho} = \frac{T_g.\left(\frac{\partial P}{\partial T_g}\right)_v + \left(fL\rho^2V^2/2D.d\rho\right)}{C_v.\rho^2} \quad (8)$$

Considering the locations 1 and 2 as the computation contours about an interval of Δx from the pipe length as shown in Fig. 1, the density variation can be expressed with the aid of eq. (4) to become:

$$d\rho = \frac{\rho_1}{V_2}.(V_1 - V_2) \quad (9)$$

Combining eqs. (8) and (9) gives :

$$\frac{dT_g}{d\rho} = \frac{T_g.\left(\frac{\partial P}{\partial T_g}\right)_v + \left(fLG^2/2D\right).\left\{V_2/[\rho_1.(V_1 - V_2)]\right\}}{C_v.\rho^2} \quad (10)$$

where $G = \rho V$ is the steam mass velocity. The Beattie - Bridgeman (BB) equation of state [9] in which pressure is explicitly expressed reads:

$$P = RT_g \rho + \beta \rho^2 + \gamma \rho^3 + \delta \rho^4 \quad (11)$$

where

$$\beta = RT_g B - A - \frac{RC}{T_g} \quad (12)$$

$$\gamma = Ad - RT_g Bb - \frac{RBC}{T_g} \quad (13)$$

$$\text{and } \delta = \frac{RBb}{T_g} \quad (14)$$

Numerical values of the five constants in eqs. (12-14) were derived by Muneer and Scott [9] as follows:

$$A = 0.769185 \quad , \quad B = 0.00126 \quad , \quad C = 930477.801426$$

$$d = 0.005318 \quad , \quad b = 0.002482.$$

To solve eq. (10) using Runge-Kutta method, it is required firstly that the right hand-side of this equation can be evaluated numerically. For this purpose, the differentiation $(\partial P / \partial T_g)_v$ in this equation is determined using eq. (11) to become,

$$\left(\frac{\partial P}{\partial T_g} \right)_v = R\rho + \dot{\beta} \rho^2 + \dot{\gamma} \rho^3 + \dot{\delta} \rho^4 \quad (15)$$

$$\text{where } \dot{\beta} = \frac{\partial \beta}{\partial T_g} = RB + \frac{2RC}{T_g^2} \quad (16)$$

$$\dot{\gamma} = \frac{\partial \gamma}{\partial T_g} = -RBb + \frac{2RBC}{T_g^2} \quad (17)$$

$$\text{and } \dot{\delta} = \frac{\partial \delta}{\partial T_g} = \frac{2RBbC}{T_g^2} \quad (18)$$

Secondly, an expression for C_v is required to complete the solution of eq. (10). This expression is derived herein after considering the real gas behavior of steam and following the thermodynamic approach which was discussed in [5, 11]. This approach can be employed as follows:

$$\begin{aligned}
ds &= \frac{1}{T_g} \cdot du + \frac{P}{T_g} \cdot dv \\
&= \frac{C_v}{T_g} \cdot dT_g + \left(\frac{\partial P}{\partial T_g} \right)_v \cdot dv
\end{aligned} \tag{19}$$

The entropy change during steam flow can also be expressed considering the non-ideal behaviour of steam and due to [11] as

$$ds = \left(\frac{\partial s}{\partial T_g} \right)_v \cdot dT_g + \left(\frac{\partial s}{\partial v} \right)_{T_g} \cdot dv \tag{20}$$

Bober and Chow [5] show that the mix derivatives in the last expressions must be the same regardless of the order of differentiation and consequently they derived that

$$\left[\frac{\partial}{\partial v} \left(\frac{C_v}{T} \right) \right]_T = \left[\frac{\partial}{\partial T} \left(\frac{\partial P}{\partial T} \right)_v \right]_v$$

Therefore,

$$\frac{1}{T_g} \cdot \left(\frac{\partial C_v}{\partial v} \right) = \left(\frac{\partial^2 P}{\partial T_g^2} \right)_v \tag{21}$$

Integration of eq. (21) at constant steam temperature and from specific volume at zero pressure to any specific volume yields

$$C_v(T_g, \rho) - C_{v0}(T_g) = T_g \int_{\infty}^v \left(\frac{\partial^2 P}{\partial T_g^2} \right)_v \cdot dv \tag{22}$$

where $C_{v0}(T_g)$ is the zero pressure specific heat capacity at constant volume.

The heat capacities can be expressed at zero pressure, where the ideal gas conditions prevail, by

$$C_{v0}(T_g) = C_{p0}(T_g) - R \tag{23}$$

At this point, an empirical equation for $C_{p0}(T_g)$ is used here. This equation was presented by Keenan, et al. [7] and adopted by Young [12] as

$$C_{p0}(T_g) = \sum_{i=1}^6 a_i T_g^{i-2} \tag{24}$$

With T_g in K and $C_{po}(T_g)$ in kJ/kg.k, the constants a_i are reported in [11]. The calculation of eq.(22) requires the evaluation of the second order derivative $(\partial^2 P / \partial T_g^2)_v$. This can be determined referring to eq. (15) by

$$\left(\frac{\partial^2 P}{\partial T_g^2} \right)_v = \ddot{\beta} \rho^2 + \ddot{\gamma} \rho^3 + \ddot{\delta} \rho^4 \quad (25)$$

where

$$\ddot{\beta} = \frac{\partial \dot{\beta}}{\partial T_g} = -\frac{6RC}{T_g^4} \quad (26)$$

$$\ddot{\gamma} = \frac{\partial \dot{\gamma}}{\partial T_g} = -\frac{6RBC}{T_g^4} \quad (27)$$

$$\text{and } \ddot{\delta} = \frac{\partial \dot{\delta}}{\partial T_g} = -\frac{6RBbC}{T_g^4} \quad (28)$$

Integration of eq. (22) with the aid of eq. (25) gives

$$C_v(T_g, \rho) - C_{vo}(T_g) = T_g \cdot \left(\rho \ddot{\beta} + \frac{\rho^2}{2} \ddot{\gamma} + \frac{\rho^3}{3} \ddot{\delta} \right) \quad (29)$$

Now, equation (10) is ready to be solved numerically using Runge-Kutta method.

In conclusion, the above formulation is based upon expressing the first order derivative $(\partial P / \partial T_g)_v$ and the second order one $(\partial^2 P / \partial T_g^2)_v$ using the investigated equation of state. Therefore, to examine the effect of state equation type, new formulations for the derivatives $(\partial P / \partial T_g)_v$ and $(\partial^2 P / \partial T_g^2)_v$ are released using the other equation of steam state (i.e., the second virial equation).

The second virial (SV) equation of state was suggested by Keenan and others [7] as :-

$$P = \rho RT_g (1 + \alpha \rho) \quad (30)$$

$$\text{where : } \alpha = C_1 - \frac{C_2 10^{[K_1 / (K_2 + T_g^2)]}}{T_g} \quad (31)$$

In the above equations (30-31), the numerical values of constants C_1 , C_2 , K_1 & K_2 are taken due to [7] as :

$$C_1 = 2.0624 \times 10^{-3} \quad , \quad C_2 = 2.61204$$

$$K_1 = 100800 \quad , \quad K_2 = 34900$$

In carrying out the required derivatives, a similar procedure to that carried out with (BB) equation is applied here. The first order derivative $\left(\frac{\partial P}{\partial T_g}\right)_v$ can readily be obtained from eqs. (30-31) as

$$\left(\frac{\partial P}{\partial T_g}\right)_v = R\rho + \alpha R\rho^2 + \dot{\alpha} R T_g \rho^2 \quad (32)$$

where : $\dot{\alpha} = \frac{\partial \alpha}{\partial T_g}$

$$= \frac{2C_2 K_1 \ln 10}{(K_2 + T_g^2)^2} \cdot 10^{[K_1/(K_2 + T_g^2)]} + \frac{C_2 \cdot 10^{[K_1/(K_2 + T_g^2)]}}{T_g^2} \quad (33)$$

Similarly as eqs. (25-28), the second order derivative is expressed by :

$$\left(\frac{\partial^2 P}{\partial T_g^2}\right)_v = 2\ddot{\alpha} R\rho^2 + \ddot{\alpha} R T_g \rho^2 \quad (34)$$

where : $\ddot{\alpha} = \frac{\partial \dot{\alpha}}{\partial T_g}$

$$= - \left\{ C_3 \cdot \frac{T_g \cdot 10^{[K_1/(K_2 + T_g^2)]}}{(K_2 + T_g^2)^4} + C_4 \cdot \frac{T_g \cdot 10^{[K_1/(K_2 + T_g^2)]}}{(K_2 + T_g^2)^3} \right\} - \left\{ C_5 \cdot \frac{10^{[K_1/(K_2 + T_g^2)]}}{T_g \cdot (K_2 + T_g^2)^2} + 2C_2 \cdot \frac{10^{[K_1/(K_2 + T_g^2)]}}{T_g^3} \right\} \quad (35)$$

$$, C_3 = 4C_2 \cdot K_1^2 (\ln 10)^2$$

$$, C_4 = 8C_2 \cdot K_1 (\ln 10)$$

$$, C_5 = 2C_2 \cdot K_1 (\ln 10)$$

Introducing the above expression for $\left(\frac{\partial^2 P}{\partial T_g^2}\right)_v$, i.e. eqs. (34-35), into eq. (22) can release the following formulation for steam specific heat capacity at constant volume

$$C_v(T_g, \rho) - C_{vo}(T_g) = -T_g(2\dot{\alpha}R\rho + \ddot{\alpha}RT_g\rho) \quad (36)$$

In order to use concept of Mach number during the solution procedure or in exposing the model results, a knowledge about the speed of sound in steam must be needed here. This speed can be defined due to [11] by

$$a_g^2 = \left(\frac{\partial P}{\partial \rho}\right)_s = -v^2 \left(\frac{\partial P}{\partial v}\right)_s \quad (37)$$

Basically, the term $(\partial P/\partial v)_s$ is obtained using BB equation to give

$$\left(\frac{\partial P}{\partial v}\right)_s = -\frac{RT_g}{v^2} + \frac{R}{v} \left(\frac{\partial T_g}{\partial v}\right)_s - \frac{2\beta}{v^3} - \frac{3\gamma}{v^4} - \frac{4\delta}{v^5} \quad (38)$$

and using SV equation to obtain :

$$\left(\frac{\partial P}{\partial v}\right)_s = -\frac{RT_g}{v^2} + \frac{R}{v} \left(\frac{\partial T_g}{\partial v}\right)_s - \frac{2\alpha RT_g}{v^3} + \frac{\alpha R}{v^2} \left(\frac{\partial T_g}{\partial v}\right)_s \quad (39)$$

Thermodynamically, the derivative $(\partial T_g/\partial v)_s$ is defined by

$$\left(\frac{\partial T_g}{\partial v}\right)_s = -\frac{T_g}{C_v} \left(\frac{\partial P}{\partial T_g}\right)_v \quad (40)$$

Differentiation of P in BB & SV equations with T_g in a constant volume is given above by equations (15) and (32). Substituting equations (15) and (32) into equations (38) and (39) respectively and taking into account the relation (40) during this substitution gives for utilization BB equation the following

$$\begin{aligned} \left(\frac{\partial P}{\partial v}\right)_s &= -\frac{RT_g\rho^2}{C_v} (C_v + R + \beta\rho + \dot{\gamma}\rho^2 + \dot{\delta}\rho^3) \\ &\quad - \rho^3(2\beta + 3\gamma\rho + 4\delta\rho^2) \end{aligned} \quad (41)$$

and on using SV equation the following relation results:

$$\begin{aligned} \left(\frac{\partial P}{\partial v}\right)_s &= -RT_g\rho^2(1+2\alpha\rho) - \frac{R^2T_g\rho^2}{C_v}(1+\alpha\rho)^2 \\ &\quad - \frac{\dot{\alpha}R^2T_g\rho^3}{C_v}\rho^3(1+\alpha\rho) \end{aligned} \quad (42)$$

Substituting eqs. (41) and (42) into eq. (37) gives :

$$a_g^2 = \frac{RT_g}{C_v} (C_v + R + \beta\rho + \gamma\rho^2 + \delta\rho^3) + (2\beta\rho + 3\gamma\rho^2 + 4\delta\rho^3) \quad (43)$$

$$\text{and } a_g^2 = RT_g(1 + 2\alpha\rho) + \frac{\alpha R^2 T_g^2 \rho}{C_v} (1 + \alpha\rho) + \frac{R^2 T_g}{C_v} (1 + \alpha\rho)^2 \quad (44)$$

, respectively.

Equation (43) is used in obtaining the speed of sound when model prediction follows BB equation, while eq. (44) is used with SV equation computation.

Therefore, after obtaining the square roots of eqs. (43 or 44); i.e. sound speed; the steam Mach number is calculated from

$$M_g = \frac{V}{a_g} \quad (45)$$

Before starting the calculations, it is necessary to specify an equation that combines the saturation pressure and saturation temperature of steam outside the possibilities of BB and SV equations. A convenient equation for this purpose is also taken from [7, 12] as

$$\frac{P_s}{P_c} = \exp \left[0.01 (T_c / T_s) \sum_{i=1}^8 b_i (3.3815 - T_s)^{i-1} \right] \quad (46)$$

where, $T_c = 647.286$ K, $P_c = 220.98$ bar and the constants b_i are given in [7,12].

SOLUTION PROCEDURE

A computer program was developed and executed to solve eq. (10) and the required supplementary equations. The solution has begun by assigning initial values to the variable flow parameters ahead of the pipe entrance. Numerical integration of eq. (10) is carried out using Runge-Kutta method. This integration was carried out for a pipe of a known geometry with finite step size. Through each step of computations, an infinitesimal difference in steam density as an independent variable was considered to obtain a new value of ρ after the integration or behind the step. The density change for each step is specified in accordance with the number of steps, initial density and the expected or measured final density. Therefore, a new value of steam temperature behind the step is specified after integration. The new values of T_g and ρ are directed to calculate a new value of steam pressure through this step using BB equation or SV equation. The flow properties for the ideal case are determined simply by setting the constants of BB and SV equations equal to zero (i.e., reducing BB or SV equation to be that of ideal gas).

EXPERIMENTAL WORK

One aim of this study was to obtain experimental data for steam flow through a pipe of definite geometry. This was necessary to verify the numerical results of the present model. Accordingly, an experimental set-up was built, tested and operated. This set-up consists mainly, as shown diagrammatically in Fig. 2, of a fire tube boiler, a piping system, the test pipe section and a surface condenser. The boiler delivers wet steam with wetness fraction of 0.5% at a rate of one ton per hour and a pressure of 6.0 bar. The test pipe is a commercial seamless pipe of 0.05 m inner diameter and 1.0 m long, ($L/D=20$).

Two pressure transducers were used to obtain the pressure values at the inlet and exit sections of the tested pipe. The dryness fraction and static temperature of supplied steam to the tested pipe were measured using a throttling calorimeter and a thermocouple, respectively. Mass flux of the flowing steam was rated after complete condensation in the condenser using a metering tank.

RESULTS AND DISCUSSION

The numerical results of present investigation are divided into three groups. In the first one, where the effect of state equation type is presented, the dimensionless values of P/P_i and T_g/T_{gi} are plotted against steam Mach number (M_g) in Fig.3. Whilst the other two groups deal with the effects of initial flow parameters (P_i and T_{gi}) and pipe geometry characteristics (f and D) on the behavior of steam flow are shown in figures 4 through 7. These two groups are illustrated here as dimensionless values of P/P_i , T_g/T_{gi} and M_g versus dimensionless pipe length L/D . It is of great importance to note that all the boundary conditions considered during program computations are listed also on Figs.3-7. These results, i.e. of Figs.3-7, were obtained for steam flow through a pipe of $D = 0.05\text{m}$ and $L = 20 D$.

Figure 3 shows the effect of the type of the state equation on the variation of steam flow characteristics along the tested pipe. From this figure it is clear that, the pressure variation with steam Mach number is less sensitive to changing the type of the state equation than the temperature variation. This tendency was concluded in many of the standard textbooks. Therefore, this tendency is explained now considering the concept illustrated by Shapiro [12] for the flow of a perfect gas in constant area ducts. Shapiro's correlations for the pressure and temperature variations along the duct reveals that the pressure variation equals the magnitude of temperature variation with the power 0.5. This causes the values of T_g/T_{gi} be greater than the corresponding values of P/P_i at a certain Mach number and consequently diverges the differences between the predicted T_g/T_{gi} for the investigated state equations.

The diagrams of Fig. 4 show the effect of changing steam flow initial pressure on the variation of the flow characteristics along the tested pipe. These diagrams were taken using both SV and BB equations. An overview of the results of Fig. 4 indicates that increasing the steam flow initial pressure tends to

decrease both the predicted P/P_i and T_g/T_{g_i} along the pipe and consequently increasing the flow Mach number. However, it is apparent from Fig. 4 that the differences between the predicted values of P/P_i and T_g/T_{g_i} using SV and BB equations are very small and that the two equations can predict the same values of M_g along the pipe. In this sense, the remainder conditions of the numerical results were carried out using BB equation only. Figures 5.a, 5.b and 5.c depict the effect of changing steam initial temperature on the behaviour of flow characteristics through a pipe having dimensions as presented above. It is obvious here that the steam temperature has been taken constant during the flow within the pipe. This flow behaviour has been developed when a gas flows at low velocities in a long duct through which heat transfer can occur readily and consequently the flow conditions may be approximately isothermal. However, it is apparent that increasing initial steam temperature increases the total pressure and temperature drops and consequently increases the Mach number of the steam flow through the pipe. This is because as the steam temperature increases, the steam viscosity will; therefore; increase [7]. Basically, the pressure drop of isothermal flow of a compressible fluid in a pipeline was found to be a function of the fluid viscosity. Therefore, the steam pressure drop along a pipe increases as the steam temperature and consequently the steam viscosity increases. Furthermore, there are another explanation for the tendency of steam pressure drop and steam temperature drop variations in Figs. 5.a and 5.b as given herein after using the analytical approach presented in [1] for the hydrodynamic calculations of steam and gas pipelines. In this approach, it was found that both the pressure drop and temperature drop accompanying steam flow through a pipe depends on steam mass velocity, steam specific volumes at pipe inlet and its exit and pipe dimensionless resistance coefficient. Only the steam specific volumes between these parameters were found to be affected with changing the steam initial temperature. Thus, as the steam temperature increases; the steam specific volumes increase and tend to increase the steam pressure drop between the inlet and exit sections of the pipe.

The next issue to be addressed in the results of present model is the effect of pipe geometry characteristics (i.e., friction coefficient of steam flow through the pipe and the pipe diameter) on the parameters of flow behaviour that used above. In considering this issue, diagrams for the behaviour of steam flow through the investigated pipes are given in Figs. 6 and 7. As can be seen in Fig. 6, increasing the friction coefficient of the steam flow through the pipe tends to decrease both the pressure and temperature of the steam and therefore increasing the steam Mach number along the pipe. This was also confirmed in [13]. In Fig. 7, effect of pipe size variation on the predicted P/P_i , T_g/T_{g_i} and M_g is given for pipes with different internal diameters and a constant length. As can be seen from Fig. 7, decreasing the pipe internal diameter causes both the predicted pressure drop and temperature drop of the steam flow along these pipes to increase. This leads to increase the steam Mach number in these pipes. This is due to the fact that decreasing the pipe internal diameter causes Reynolds number of the steam flow to increase. Accordingly, pressure losses

increase in different proportions to Reynolds number as was concluded in many of the textbooks and handbooks.

In order to discuss the effectiveness of the present model, the predicted results of this model are compared to experimental ones. Figure 8 illustrates a comparison between measured pressure drops in steam flow through pipes and the corresponding theoretical findings obtained using present model. Experimental results in Fig.8.a are due to present measurements, while that of Fig. 8.b are due to Manzano-Ruiz, et. al.[14]. Boundary conditions of the experiments and pipes geometry are presented in Fig.8. Based on this figure, it is clear that the computed results of the steam flow pressure drop over the whole length of the tested pipes agreed well with the measurements of present experiments (error=0.4%) as well as with the experimental data of Manzano-Ruiz, et. al.[14] (0.75% error).

CONCLUSION

In the present study, a theoretical model has been illustrated utilizing two equations for steam state namely Beattie-Bridgeman (BB) and second virial (SV) equations in order to predict the real characteristics of steam flow through pipes. The numerical results demonstrate the effects of considering real gas aspects, initial flow parameters and pipe geometry characteristics on the behaviour of steam flow through pipes. Results discussion reveals that the utilized state equations, i.e. BB and SV equations, predict closely the same values of steam flow characteristics. This yields that each of BB equation or SV equation can similarly simulate the real medium characteristics of steam flow through pipes. Furthermore, model predictions show that varying some of the initial conditions of steam flow ahead the pipe inlet as well as changing the pipe geometrical characteristics can affect the total pressure drop, temperature drop and Mach number of steam flow through the pipe. Finally and of considerable practical importance, the experimental and theoretical results of the present work indicate that if high accuracy is required in determining steam flow characteristics through a pipe there is no limitation for the range of steam conditions in applying the present model. With this model, the characteristics of steam flow through pipes are well predicted.

REFERENCES

- [1] Rudomino, B. and Remzhin, Yu., Steam Power Plant Piping Design, Mir Publishers, Moscow, 1979.
- [2] Chisholm, D., Pressure gradients due to friction during the flow of evaporating two-phase mixtures in smooth tubes and channels, Int. J. Heat Mass Transfer, Vol. 16, pp. 347-358, 1973.
- [3] Chisholm, D., Influence of pipe surface roughness on friction pressure gradient during two-phase flow, J.Mech.Eng. Science, Vol. 20, NO. 6, pp. 353-354, 1978.

- [4] Sullivan, D.A., Historical review of real-fluid isentropic flow models, ASME J. Fluids Eng., Vol. 103, pp. 258-266, 1981.
- [5] Bober, W. and Chow, W.L., Non-ideal isentropic gas flow through converging-diverging nozzles, ASME J. Fluids Eng., Vol. 112, pp. 455-461, 1990.
- [6] Bober, W. and Chow, W.L., Non-ideal gas effects for the venturi meter, ASME J. Fluids Eng., Vol. 133, pp. 301-304, 1991.
- [7] Keenan, J.H., Keyes, F.G., Hill, P.G. and Moore, J.G., Steam Tables, John Wiley and Sons, New York, 1969.
- [8] Bakhtar, F., Ryley, D.J., Tubman, K.A. and Young, J.B., Nucleation studies in flowing high pressure steam, Proc. Instn Mech. Engrs, Vol. 189, pp. 427-436, 1975.
- [9] Sabry, T.I., Khalifa, B.A., Ibrahim, K.A. and Mahmoud, N.H., Nonequilibrium condensing wet steam flow through nozzles, Eng. Research Bull., Menoufia University, Egypt, Vol. X, Part I, pp. 87-106, 1988.
- [10] Muneer, T. and Scott, S.M., The calculation of thermodynamic properties of steam for minimum computer access time, Proc. Instn Mech. Engrs, Vol. 105, pp. 25-29, 1991.
- [11] Kirillin, V.A. Sychev, V.V. and Sheindlin, A.E., Engineering Thermodynamics, Mir Publishers, Moscow, 1976.
- [12] Young, J.B., An equation of state for steam for turbomachinery and other flow calculations, ASME J. Eng. for Gas Turbines and Power, Vol. 110, pp. 1-7, 1988.
- [13] Shapiro, A.H., The Dynamics and Thermodynamics of Compressible Fluid Flow, Vol. I, Roland Press Comp., New York, 1953.
- [14] Manzano-Ruiz, J.J., Hernandez, A., Grases, P., Zagustin, K., Kastner, W., Kefer, V., Koehler, W. and Kraetzer, W., Pressure-drop in steam-water flow through large bore horizontal piping, paper E1, pp. 139-147, Proceedings of the 3rd Int. Conf. on Multiphase flow, the Hague, the Netherlands, 1987.

NOMENCLATURE

| | | |
|---------------------------|---|----------------------|
| a_2 | speed of sound. | m/s |
| A | cross-sectional area of the pipe. | m ² |
| C_p | isobaric specific heat capacity of steam. | kJ/kg.K |
| C_v | isochoric specific heat capacity of steam. | kJ/kg.K |
| C_1, C_2, C_3, C_4, C_5 | constants in eqs. (31-35) | -- |
| D | pipe inner diameter. | m |
| f | friction coefficient of steam flow through the pipe | -- |
| G | steam mass flux. | kg/m ² .s |
| h | specific enthalpy. | kJ/kg |

| | | |
|-------------------------|-------------------------------|--------------------|
| K_1, K_2 | constants in eq. (31) | -- |
| L | pipe length. | m |
| M_g | steam Mach number | -- |
| P | pressure. | bar |
| R | gas constant (=461.51.) | J/kg.K |
| s | specific entropy. | kJ/kg.K |
| T | temperature. | K |
| T_g | steam temperature. | K |
| T_s | steam saturation temperature. | K |
| v | specific volume. | m ³ /kg |
| V | mean steam velocity | m/s |
| x | distance in flow direction. | m |
| α | second virial coefficient. | m ³ /kg |
| β, γ, δ | constants in BB equation. | -- |
| ρ | density. | kg/m ³ |

SUBSCRIPTS

| | |
|---|--|
| c | critical conditions |
| g | steam. |
| i | initial or stagnation conditions. |
| O | at zero pressure. |
| P | constant pressure. |
| s | saturation conditions or constant entropy. |
| v | constant volume. |

ABBREVIATIONS

| | |
|----|---------------------|
| BB | Beattie - Bridgeman |
| SV | second virial. |

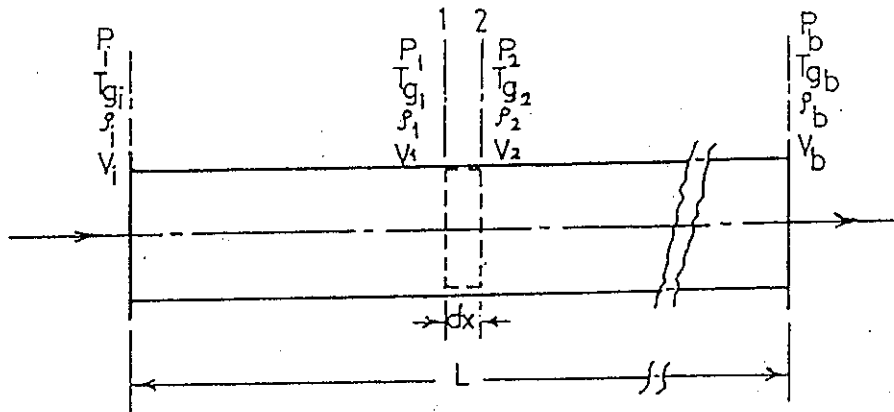
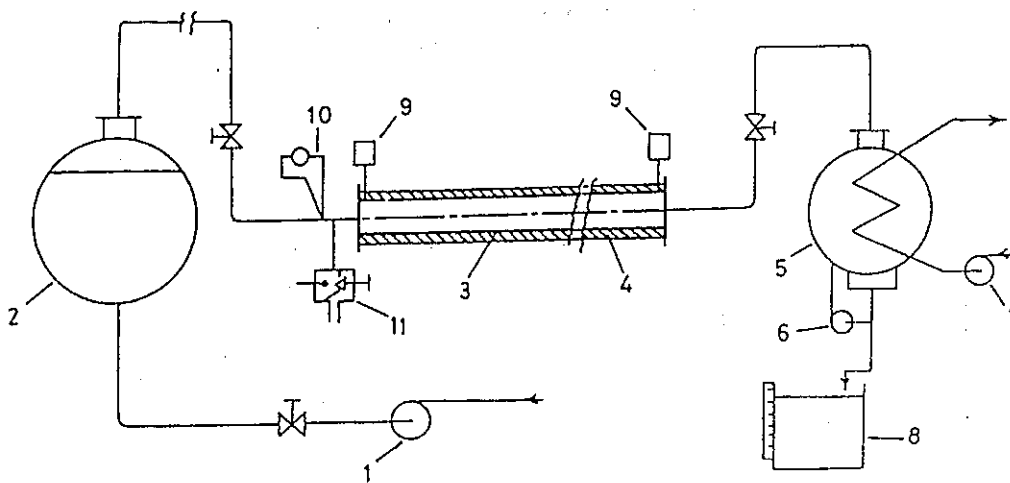


Fig. 1 Variation of steam properties across an element of flow configuration through a pipe.



- | | |
|----------------------|---------------------------|
| 1 Feed Pump | 7 Circulating Pump |
| 2 Steam Boiler | 8 Metering Tank |
| 3 Tested Pipe | 9 Pressure Transducer |
| 4 Thermal Insulation | 10 Thermocouple |
| 5 Condenser | 11 Throttling Calorimeter |
| 6 Vacuum Pump | |

Fig. 2 Schematic of the experimental set-up.

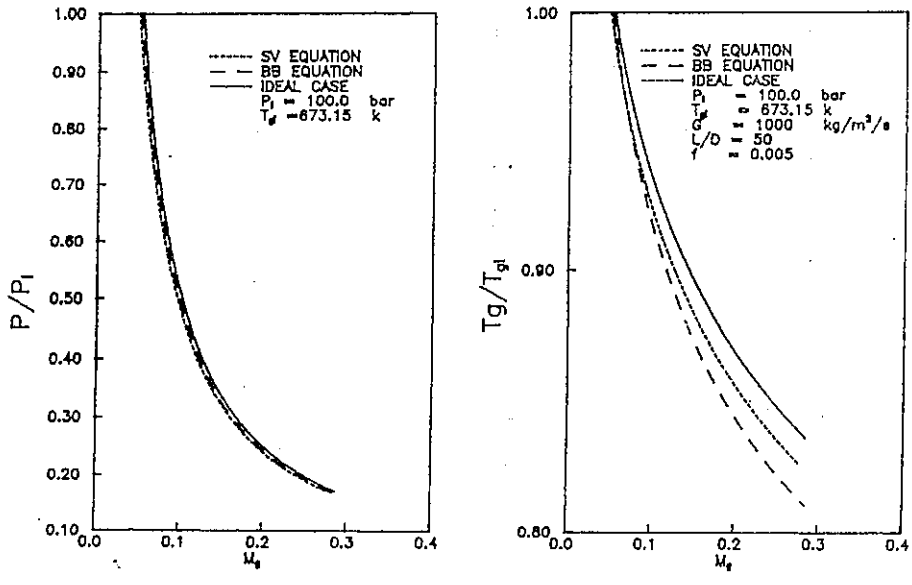


Fig. 3 Effect of state equation type on the variation of steam flow characteristics through a 50 mm diameter pipe of $L/D = 50$.

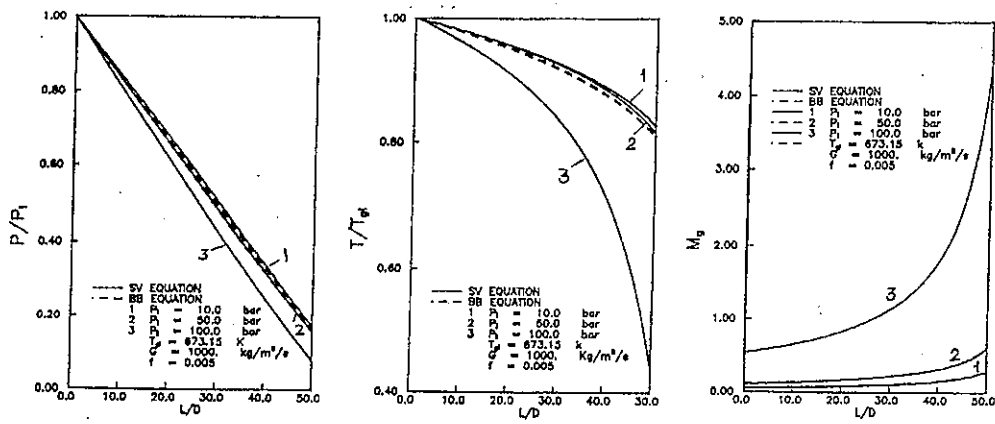


Fig. 4 Effect of steam initial pressure on the variation of flow characteristics along a pipe.

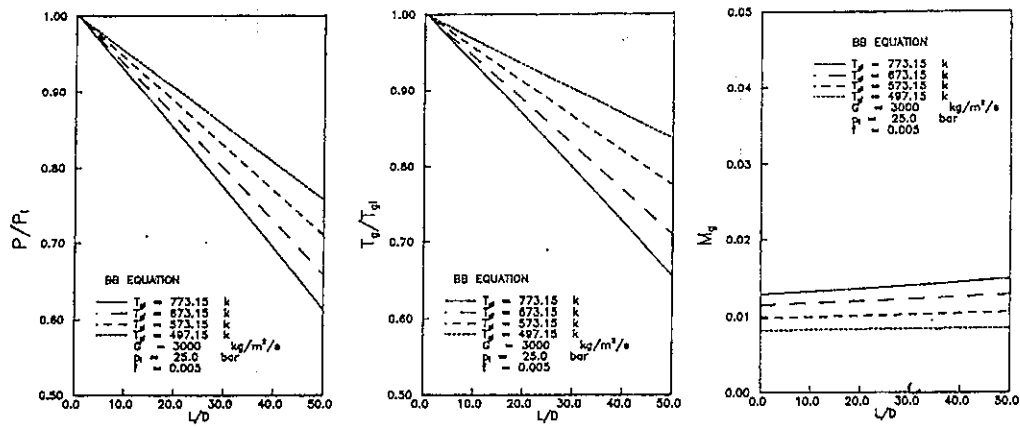


Fig. 5 Effect of steam initial temperature on the variation of flow characteristics along pipes.

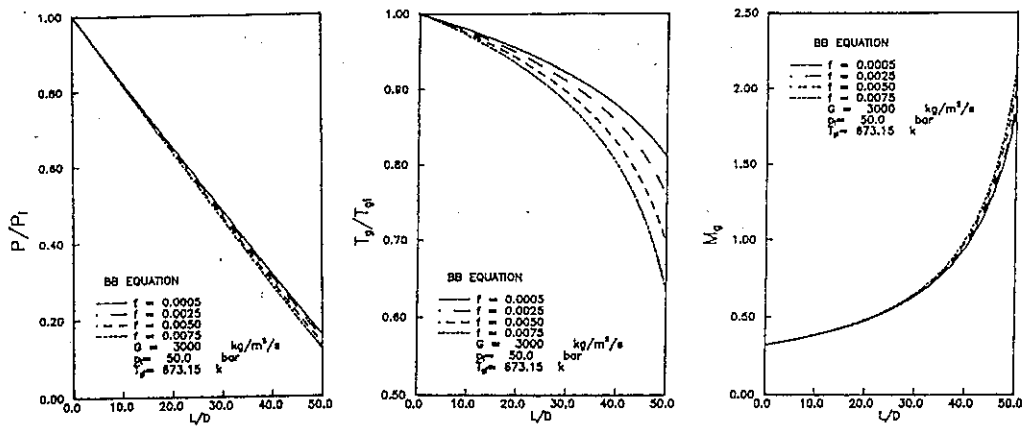


Fig. 6 Effect of friction coefficient variation on the predicted steam flow characteristics along pipes.

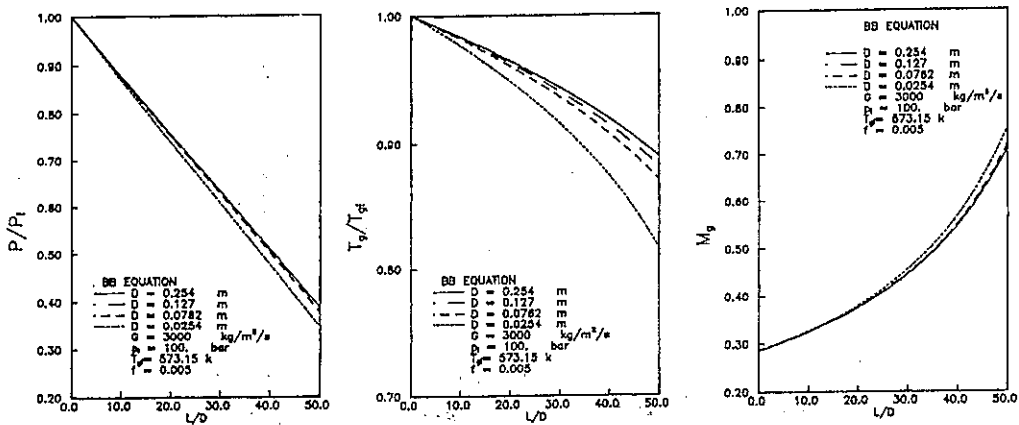


Fig. 7 Effect of pipe size (D) on the predicted steam flow characteristics through pipes.

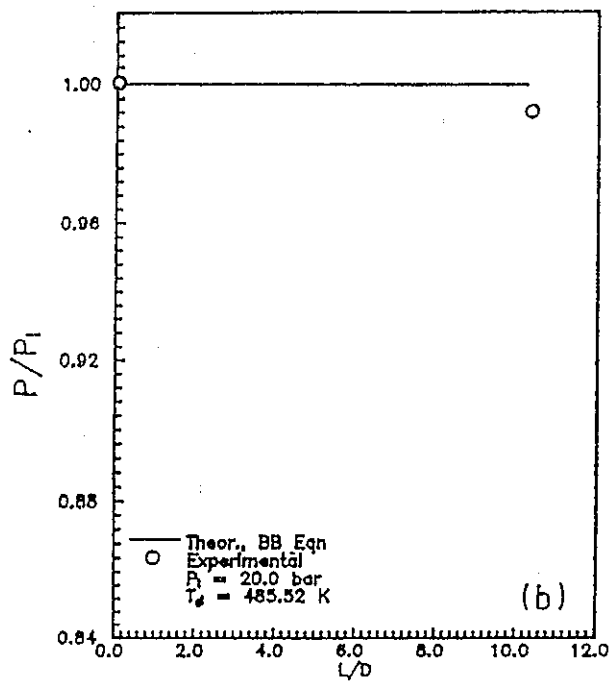
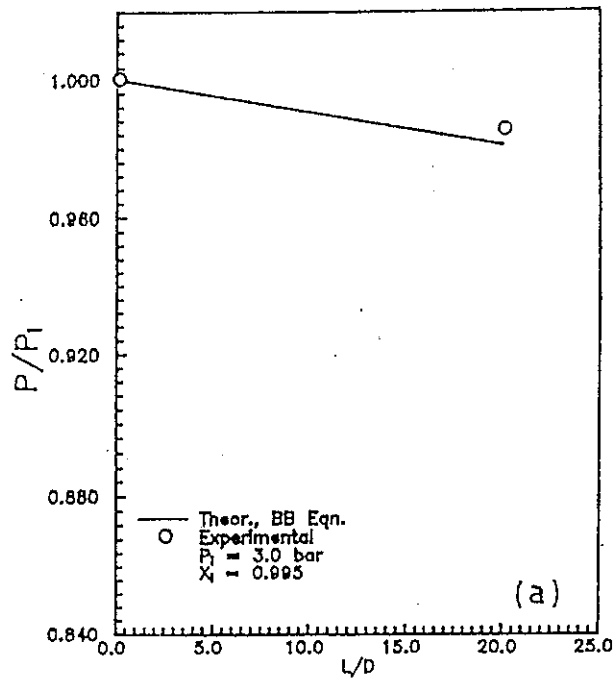


Fig. 8 A comparison between predicted and measured values of steam flow pressure along pipes.
 a- present experiment on a horizontal pipe of $D \approx 0.05$ m and $L \approx 1.0$ m.
 b- experiment due to Manzano-Ruiz, et al. [14] per 1.0 m length from a horizontal pipe of 0.097m diameter.

بِسْمِ اللَّهِ الرَّحْمَنِ الرَّحِيمِ

الملخص العربى

نموذج نظري لتقييم تأثيرات المائع الحقيقى لتدفق البخار خلال الأنابيب.

د. نبيل حنفى محمود - د. عاشور عبد الفتاح خطاب

قسم هندسة القوى الميكانيكية - كلية الهندسة - جامعة المنوفية

تصف هذه الورقة نمودجا نظريا يأخذ فى الإعتبار تأثيرات المائع الحقيقى فى الخصائص المميزة لتدفق البخار خلال الأنابيب عند ضغوط عالية - متوسطه ومنخفضة، يستخدم هذا النمودج معادلتى حاله شائعتى الإستعمال وهما معادلة باتى-برد جمان ومعادلة من النوع الثنائى الشطرات، تم إستخدام معادلات أساسية معدلة وذلك لضم تأثير خشونة الأنبوبة فى اشتقاق النمودج الرياضى، تم الحصول على توقعات لتغيرات الضغط-درجة الحرارة ورقم الماخ لتدفق البخار خلال أنبوية ذات شكل هندسى معين بإستخدام طريقة رانج-كوتا فى حل المعادلات التفاضلية للنمودج، كذلك فقد تضمن مخطط النتائج التغيرات فى بارامترات تدفق البخار والمناظرة لإستعمال معادلة الحالة لغاز مثالى فى النمودج.

تم إجراء برنامج معملى وذلك للحصول على معطيات معملية، لقد توافقت النتائج المحسوبة للهبوط فى ضغط تدفق بخار على طول انبوية جيداً مع القياسات من تجارب البحث الحالى مثلما توافقت مع المعطيات المعملية المذكورة فى الأعمال السابقة.

1. The first part of the document discusses the importance of maintaining accurate records of all transactions and activities. It emphasizes that this is essential for ensuring transparency and accountability in the organization's operations.

2. The second part of the document outlines the various methods and tools used to collect and analyze data. It highlights the need for consistent and reliable data collection processes to support effective decision-making.

3. The third part of the document focuses on the role of technology in data management and analysis. It discusses how modern software solutions can streamline data collection, storage, and reporting, thereby improving efficiency and accuracy.

4. The fourth part of the document addresses the challenges associated with data management, such as data quality, security, and privacy. It provides strategies to mitigate these risks and ensure that data is used responsibly and ethically.

5. The fifth part of the document concludes by summarizing the key findings and recommendations. It stresses the importance of ongoing monitoring and evaluation to ensure that data management practices remain effective and aligned with the organization's goals.

CONCLUSION

In conclusion, the document has provided a comprehensive overview of the data management process. It has highlighted the significance of accurate data collection and analysis, the role of technology, and the challenges that must be addressed to ensure data integrity and security. The recommendations provided are intended to guide the organization in implementing best practices for data management.